

# The reactions of $\text{NO}_2$ and $\text{CH}_3\text{CHO}$ with Na-Y zeolite and the relevance to plasma-activated lean $\text{NO}_x$ catalysis

Thomas M. Orlando<sup>a,\*</sup>, Alex Alexandrov<sup>a</sup>, Andrew Lebsack<sup>a</sup>,  
Janine Herring<sup>a</sup>, John W. Hoard<sup>b</sup>

<sup>a</sup> School of Chemistry and Biochemistry, Georgia Institute of Technology, Atlanta, GA 30332, USA

<sup>b</sup> Chemical Engineering Department, Ford Motor Company, Dearborn, MI 48121, USA

## Abstract

We have examined the interaction of  $\text{NO}_2$  and  $\text{CH}_3\text{CHO}$  with Na-Y zeolite under conditions relevant to low-temperature plasma-activated reduction of  $\text{NO}_x$ . Acetaldehyde interacts weakly with the surface primarily via electrostatic and ion–dipole interactions and is not present at appreciable levels in the molecular adsorbed state at temperatures exceeding 350 K. The interaction of  $\text{NO}_2$  with Na-Y zeolite produces various forms of adsorbed nitrogen oxide species that are primarily present in the form of nitrites and nitrates. The nitrites can be present in the nitrito ( $-\text{O}-\text{N}-\text{O}^-$ ) and nitro ( $-\text{NO}_2^-$ ) configurations and nitrates in the ( $-\text{NO}_3^-$ ) and nitrate ( $-\text{O}-\text{NO}_2^-$ ) configurations. Reactions of  $\text{NO}_2$  with a Na-Y zeolite surface containing pre-adsorbed acetaldehyde at room temperature are primarily limited to oxidation of the organic fragments and reduction of the surface nitrates to surface nitrites. Reactions of  $\text{NO}_2$  on Na-Y zeolite surfaces containing a low coverage of acetaldehyde at temperatures  $>350$  K produces a dehydrogenated surface adsorbed species that likely contains C, N and O. This deposit or adsorbate is also produced when the surface is directly dosed with nitromethane and isopropyl nitrate. The surface reactions seem to involve the Al and associated acid sites. © 2003 Elsevier B.V. All rights reserved.

**Keywords:**  $\text{NO}_2$ ;  $\text{CH}_3\text{CHO}$ ; Na-Y zeolite

## 1. Introduction

In the early to mid-1990s, a relatively small group of investigators began to aggressively investigate the potential role of “plasma-activated” catalysis in the remediation of gas-phase pollutants and combustion exhaust streams [1–15]. Initially, the focus was on understanding the detailed gas-phase physical and chemical processes typical of dielectric barrier discharge devices. Penetrante was at the forefront of the modeling activities and the comprehensive body of information provided by he and his collaborators paved the path towards studies on the interaction of plasma generated species with catalyst materials either positioned within the plasma or downstream from it. Indeed, Penetrante was one of the leaders who helped develop the general field of plasma-activated catalysis and his contributions were immeasurable.

Eventually, experimental advances were made which indicated that including catalysts either within the plasma

or downstream from the plasma lead to better efficiencies and sometimes entirely different product distributions [4–15]. Several recent studies have shown that  $\text{NO}_x$  can be reduced in simulated diesel and lean-burn exhaust when utilizing low-temperature plasmas in conjunction with certain catalytic materials. Of particular relevance to the work described in this paper are early reports that some zeolite catalysts that are inactive in  $\text{NO}_x$  reduction under thermal conditions, show high activity when preceded by a low-temperature plasma device [6–8]. The gas-phase chemical kinetics models of Penetrante et al. [16] and Kushner and coworkers [17] indicated that plasma treatment of oxygen rich exhaust streams primarily oxidizes NO to  $\text{NO}_2$  and also partially oxidizes the hydrocarbons to reactive species such as RO, ROO and stable products such as acetaldehyde and formaldehyde. In principle, these species can then react on a surface forming intermediate complexes that rearrange to eventually form  $\text{N}_2$ . The mechanisms and rates of formation and decomposition of these intermediate complexes depend upon the details of the chemical composition, geometric and electronic structure and surface properties of zeolite materials. Despite this fact, no direct probing of the nature of the active sites, the identity of the reactive

\* Corresponding author. Tel.: +1-404-894-4012;  
fax: +1-404-894-7452.

E-mail address: [thomas.orlando@chemistry.gatech.edu](mailto:thomas.orlando@chemistry.gatech.edu) (T.M. Orlando).

intermediates and the kinetics of the chemical conversion to the final  $\text{N}_2$  product have been carried out. This level of information, though fundamental, is critical to developing an understanding of the catalysis operative in this novel technology. This paper reports results of an investigation of the interaction of  $\text{NO}_2$ , acetaldehyde and combinations of these reactants on Na-Y zeolites. The results provide insight concerning some of the reactions that can occur during the plasma-activated catalytic reduction of NO under lean-burn conditions.

## 2. Experiment

To investigate some of the reactions occurring in the plasma-activated catalytic reduction of  $\text{NO}_x$ , we studied the surface reactions *without* plasma pre-treatment by simply dosing powdered zeolite samples with acetaldehyde and/or  $\text{NO}_2$  under static and dynamic conditions. The experiments were carried out in a high-vacuum ( $10^{-8}$  to  $10^{-9}$  Torr) system (Fig. 1) with doses ranging from 0.1 to 1000 L. The vacuum system could also be used for high-pressure studies and consisted of a six-way stainless steel cube equipped with a rotatable temperature controlled (100–600 K) sample holder, a quadrupole mass spectrometer for temperature programmed desorption (TPD) and a sapphire leak valve for controlled dosing of reactants. Higher pressure studies usually involved doses of up to  $10^7$  L.

The zeolite material studied was a commercial Na-Y, FAU (CBV 100: Si/Al ratio 2.55, 13 wt.%  $\text{Na}_2\text{O}$ , unit cell size 24.65 Å, specific surface 900  $\text{m}^2/\text{g}$ ) obtained from ZEO-OLYST and the catalyst was used as-received. The Na-Y zeolite was selected because of its demonstrated efficiency

in plasma-activated catalytic conversion of nitrogen oxides. The powdered catalyst sample was deposited on a zirconium foil attached to the sample holder and the temperature was monitored with a type-K thermocouple spot welded to the zirconium. The 1 mg of zeolite powder was uniformly distributed over the 1  $\text{cm}^2$  area of the zirconium base. Assuming a specific surface area between 800 and 1000  $\text{m}^2/\text{g}$ , the whole surface of the sample studied was approximately 1  $\text{m}^2$ . After deposition, the samples were evacuated and cleaned by heating to 550–600 K for 24 h prior to each experiment. Cleanliness was checked with post-annealing TPD in vacuum ( $10^{-7}$  Torr). During the TPD, water and organic molecules (and the expected fragment masses) were monitored with the quadrupole mass spectrometer and the surfaces were found to be free of water and adsorbed hydrocarbons. This is necessary to obtain a good understanding of the primary surface reactions involved in lean  $\text{NO}_x$  treatment using Na-Y, FAU and related materials. Evacuated and annealed samples were exposed to nitrogen dioxide or acetaldehyde vapor. The pumping line was shut off and the reactants were dosed into the chamber through the controlled leak valve. The pressure, was monitored using the ionization vacuum gauge and was kept constant during the dosing period. After exposure, the reactants remaining in the gas phase were pumped out and the Fourier transform infrared (FTIR) spectrum of the sample was recorded in the reflection/absorbance mode. The reactant dose was calculated by the pressure and exposure time.

The presence of intermediate species was probed using FTIR reflectance measurements over a wide temperature range and under a variety of dosing conditions. ZnSe windows were used to provide good optical transmission and coupling of the Bruker Equinox (FTIR) spectrometer. The FTIR spectra were obtained in the reflectance mode at 4  $\text{cm}^{-1}$  resolution and are the average of 25 scans. Data were taken primarily in the range between 500 and 2000  $\text{cm}^{-1}$ . The background scan was always taken with a clean sample and thus features due to the substrate itself are automatically subtracted. Measurements were made as a function of temperature at a fixed dose and as a function of dose at a fixed temperature. Sequential doses of the reactants were usually followed by a pump-out cycle and carried out at fixed temperatures. In the case of the co-adsorption studies, the sample was first dosed with  $\text{NO}_2$  and then dosed with  $\text{CH}_3\text{CHO}$ . Similar measurements were also carried out for initial doses of  $\text{CH}_3\text{CHO}$  followed by dosing with  $\text{NO}_2$ .

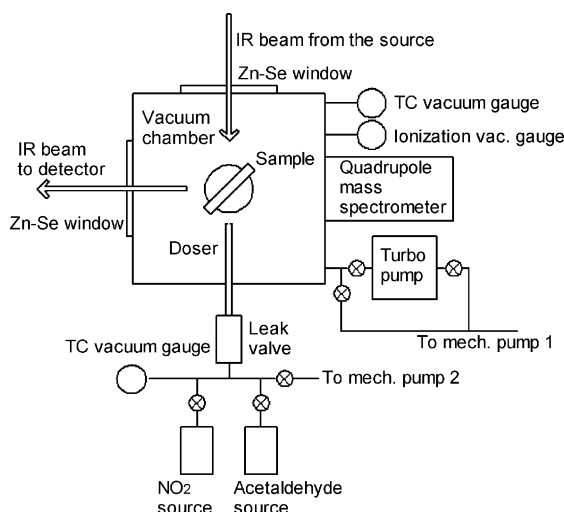


Fig. 1. Experimental setup: the sample is mounted on a rotatable temperature controlled sample holder in the high-vacuum chamber equipped with the quadrupole mass spectrometer, dosing system and zinc-selenide view ports. IR data have been obtained in both the reflection and transmission modes.

## 3. Results and discussion

### 3.1. The adsorption and interactions of acetaldehyde on Na-Y zeolites

Fig. 2 displays the FTIR spectra of acetaldehyde adsorbed on Na-Y, FAU zeolites as a function of dose at 300 K. Spec-

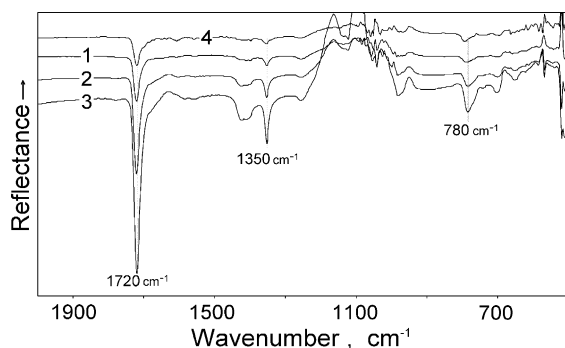


Fig. 2. The FTIR spectra of acetaldehyde adsorbed on Na-Y, FAU zeolites as a function of dosing and temperature. Spectra 1, 2 and 3 were obtained at doses of  $6 \times 10^6$  L,  $2 \times 10^7$  L and  $10^8$  L at a substrate temperature of 300 K, after that the sample was heated to 350 K (spectrum 4). Each spectrum was registered after 120 s of evacuation at 0.005 Torr. The spectra are displaced for the sake of comparison.

tra 1 and 2 correspond to acetaldehyde exposures of  $6 \times 10^6$  and  $2 \times 10^7$  L, respectively. Spectrum 3 involves approximately an order of magnitude increase in dose and spectrum 4 is the transformation of spectrum 3 after heating the sample to 350 K in vacuum at a background pressure of 0.005 Torr. Each spectrum is similar with at least three distinct sharp features at 1720, 1350 and  $780 \text{ cm}^{-1}$ . Absorption at  $1720 \text{ cm}^{-1}$  is assigned to the  $\text{R}-\text{C}=\text{O}$  stretching vibrations and the absorption in the  $1300\text{--}1400 \text{ cm}^{-1}$  region is assigned to the bending vibrations of  $\text{CH}_3$  and CH groups. Assignment of the band at  $780 \text{ cm}^{-1}$  is difficult. This band is not observed in spectra of acetaldehyde adsorbed on Na-Y zeolite at 100 K (not shown) and is probably indicative of an activated weak chemisorption state on the zeolite surface. The intensities of all bands increase with dose and the features correspond to isolated weakly adsorbed molecules. The feature perturbed the least relative to the gas-phase spectra is the  $\text{CH}_3$  deformation band at  $1350 \text{ cm}^{-1}$  so it is reasonable to infer that the methyl groups are not interacting strongly with the zeolite. The characteristic  $\text{R}-\text{C}=\text{O}$  stretching vibration around  $1720 \text{ cm}^{-1}$  has a reproducible shoulder at lower frequency. This shoulder broadens and a weak feature begins to appear with coverage around  $1600 \text{ cm}^{-1}$ . Such effects are typically associated with multiple adsorption sites in the zeolite and occur due to charge redistribution (induced dipole coupling) or partial charge transfer from the carbonyl group to a charge deficient region on/within the Na-Y zeolite.

Under the clean vacuum conditions employed in this study, the  $\text{CH}_3\text{CHO}$  is weakly coupled to the surface primarily via ion–dipole or electrostatic interactions. For example, Fig. 2, spectrum 4 demonstrates efficient desorption at a surface temperature of 350 K. We therefore conclude that acetaldehyde is rather stable on/in Na-Y and it is not present to an appreciable extent on the surface as a molecularly adsorbed species at the operating temperature ( $T > 350 \text{ K}$ ) of the secondary stage in plasma reactors.

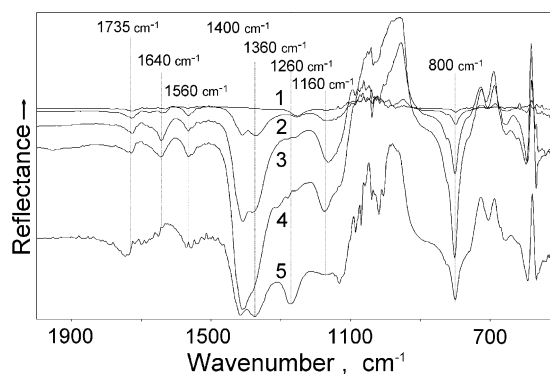


Fig. 3. The FTIR spectra of  $\text{NO}_2$  adsorbed on Na-Y, FAU as a function of dose and substrate temperature. Spectra 1, 2, 3 and 4 were obtained at doses of  $10^6$  L,  $10^7$  L,  $4 \times 10^7$  L and  $6 \times 10^8$  L at a substrate temperature of 300 K. The surface prepared for spectra 4 was then heated to 350 K to obtain spectra 5. The spectra have been displaced for the sake of comparison.

### 3.2. The adsorption and interactions of $\text{NO}_2$ on Na-Y zeolites

It is well known that  $\text{NO}_2$  interacts with metal-oxide and zeolite surfaces and leads to the formation of adsorbed nitrites and nitrates. The nitrites can be in both the nitrito ( $-\text{O}-\text{N}-\text{O}^-$ ) and nitro ( $-\text{NO}_2^-$ ) configurations and nitrates in the ( $-\text{NO}_3^-$ ) and nitrate ( $-\text{O}-\text{NO}_2^-$ ) configurations. Fig. 3, spectra 1–4 shows the FTIR spectra of  $\text{NO}_2$  adsorption on Na-Y as a function of dose at room temperature. As previously mentioned, the spectra are the differential between IR absorption of the zeolite before and after exposure to the  $\text{NO}_2$ . Therefore, the spectra do not contain any features characteristic of the substrate itself or any surface groups, such as  $-\text{OH}$ , which existed before  $\text{NO}_2$  adsorption. We assign the doublet peak at  $1400 \text{ cm}^{-1}$  to  $\text{NO}_3^-$  which is likely associated with the  $\text{Na}^+$ . The broad and intense IR features in the  $1200\text{--}1500 \text{ cm}^{-1}$  range are the composite of several  $\text{NO}_2^-$  and  $\text{NO}_3^-$  bands [18] in bridging, mono-dentate and bi-dentate bonding configurations and are more likely involved with the  $-\text{O}-\text{Si}-\text{Al}-\text{O}-$  sites comprising the zeolite framework. In particular, the feature at  $1260 \text{ cm}^{-1}$  is assigned to the  $\nu_{\text{as}}$  stretch of an adsorbed nitro ( $-\text{NO}_2^-$ ) species, whereas the feature at  $1160 \text{ cm}^{-1}$  can be assigned to the mono-dentate nitrito species coordinated on aluminum or/and silicon surface cations. Note that the very first species formed during the interaction of  $\text{NO}_2$  with the Na-Y zeolite appears around  $1240 \text{ cm}^{-1}$  and this could be associated with a chelating or bridging nitro group possibly in the nitro–nitrito configuration. The  $800 \text{ cm}^{-1}$  feature can be associated with the  $\delta(\text{N}-\text{O})$  of this bridging nitro–nitrito group. The minor features at 1735, 1640, 1560 and  $1360 \text{ cm}^{-1}$  are difficult to assign but these can be associated with adsorbed nitro-compounds, nitrogen dioxide, water, and/or organic nitro or nitrito complexes. Though this will be discussed in much more detail in Section 3.4.2, we note that the primary  $\nu(\text{R}-\text{NO}_2)$  and  $\nu(\text{R}-\text{ONO})$  bands are at

1550 and 1655  $\text{cm}^{-1}$ , respectively, and a  $\text{-CH}_3$  bending band is seen at 1360  $\text{cm}^{-1}$ . Spectrum 5 was obtained at 350 K, and though most features persist at this temperature, there is a noticeable increase in the 1735, 1360 and 1260  $\text{cm}^{-1}$  bands and an intensity loss in the 1160 and 1640  $\text{cm}^{-1}$  features.

The 1735 and 1360  $\text{cm}^{-1}$  features may be produced by the oxidation of some residual organic species and could correspond to the formation of an  $\text{R-C=O}$  containing product. This oxidation can be initiated by simple diffusion of the trace organics to the nitrate groups or the thermal degradation of the nitrate group. The latter process leads to the release of atomic and molecular oxygen and NO and  $\text{NO}_2$ . The initial formation of the nitrate may be activated since it does not occur when dosing at temperatures below 150 K (not shown). The presence of residual intrinsic water near or in contact with the Na in the pores of Na-Y is highly probable, even after annealing and heating to 500 K. The production and release of water can also accompany the formation of  $\text{NO}_x^-$  since these anions replace the surface hydroxyl groups. Thus, the formation of  $\text{NO}_x^-$  anions is either enhanced by the presence of water or associated with the production of water.

### 3.3. Acetaldehyde reactions with Na-Y, FAU pre-exposed to $\text{NO}_2$

As shown in Fig. 2, adsorption of acetaldehyde at 350 K on a freshly annealed zeolite surface forms a weakly bound layer which does not reveal any specific IR absorption spectrum other than that of the acetaldehyde itself. Interaction of acetaldehyde with the zeolite previously exposed to nitrogen dioxide significantly changes the spectrum of surface nitro-compounds (Fig. 4). In the initial sample, exposed to  $\text{NO}_2$  at 2 Torr for 300 s, a strong adsorption of surface  $\text{NO}_3^-$  groups at 1400  $\text{cm}^{-1}$  and an unassigned feature at

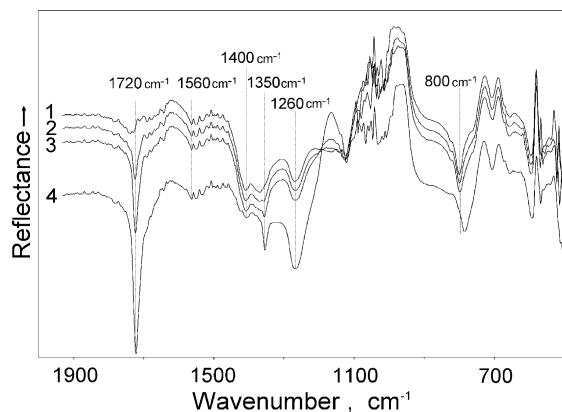


Fig. 4. Acetaldehyde reactions with Na-Y, FAU pre-exposed to  $\text{NO}_2$  at 350 K. Spectrum 1 was obtained after a 300 s dose of  $\text{NO}_2$  at 2 Torr ( $6 \times 10^8$  L) at 350 K. The surface contains a significant number of  $\text{NO}_3^-$  and  $\text{NO}_2^-$  sites. The substrate temperature was then maintained at 350 K during  $\text{CH}_3\text{CHO}$  doses. Spectra 2, 3 and 4 were obtained at doses of  $6 \times 10^6$  L,  $2 \times 10^7$  L, and  $4 \times 10^8$  L, respectively. Note the growth of the feature at 1260  $\text{cm}^{-1}$  indicating the formation of  $\text{NO}_2^-$ .

1350  $\text{cm}^{-1}$  are observed together with a less intensive peak of  $\text{NO}_2^-$  anions at 1260  $\text{cm}^{-1}$  (spectrum 1 in Fig. 4). Spectra 2 and 3 correspond to acetaldehyde dosing at 0.1 Torr partial pressure for 60 and 180 s, respectively. Neither of these spectra reveals significant changes except the ordinary growth of acetaldehyde absorptions at 1720 and 1350  $\text{cm}^{-1}$ . However, an increased dose of acetaldehyde (2 Torr for 180 s, spectrum 4) reduces absorption of  $\text{NO}_3^-$  bands by nearly a factor of 3 and increases the  $\text{NO}_2^-$  band intensity by approximately a factor of 2. No absorption bands of organic nitro or organic nitrate compounds are identified and the interaction of acetaldehyde with nitrated surfaces is probably limited to reduction of the  $\text{NO}_3^-$  to  $\text{NO}_2^-$ , and oxidation of acetaldehyde to acetate, formate or possibly carbonate.

### 3.4. $\text{NO}_2$ reactions with Na-Y, FAU pre-exposed to acetaldehyde

#### 3.4.1. Sequential adsorption of acetaldehyde and $\text{NO}_2$

The necessity of zeolite surface sites for the interaction between  $\text{NO}_2$  and acetaldehyde is clearly illustrated in the following set of experiments. The sample was saturated with acetaldehyde at 300 K by dosing at 1 Torr vapor pressure for 300 s. After evacuation to 0.005 Torr, nitrogen dioxide was dosed in the system up to 10 Torr pressure for 60 s. As illustrated in Fig. 5, spectra 1 and 2 resulting from this treatment are identical. No decrease of acetaldehyde bands is observed and only a small amount of nitro-compounds are formed at/on the surface. The lack of reactivity or inhibition can be due to several factors that include the low temperature or protection of the surface by adsorbed organic molecules. To help clarify this, a fresh zeolite was exposed to  $\text{NO}_2$  at

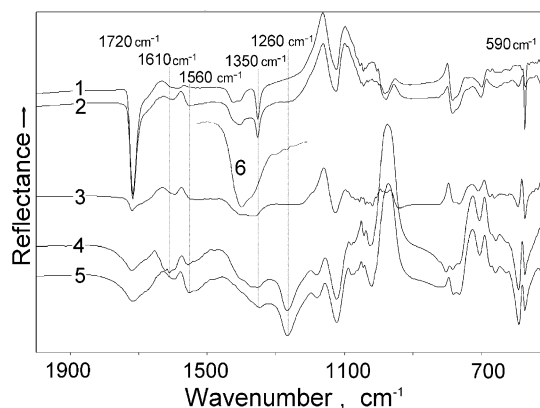


Fig. 5. Nitrogen dioxide reactions with the Na-Y zeolite with adsorbed acetaldehyde at 300 and 375 K. Spectra 1: after acetaldehyde dosing at 300 K and a vapor pressure of 1 Torr for 300 s (exposure:  $3 \times 10^8$  L). Spectra 2: the sample after previous step was exposed to  $\text{NO}_2$  at 10 Torr for 60 s ( $6 \times 10^8$  L). Spectra 3: the sample after step 2 was heated to 375 K for 300 s at a base pressure of 0.005 Torr. Spectra 4: the sample was exposed to  $\text{NO}_2$  vapor with a 2 Torr pressure for 180 s ( $3.6 \times 10^6$  L) at 375 K; spectra is registered with nitrogen dioxide in the gas phase. Spectra 5: same as spectra 4 after 300 s of evacuation at 375 K. Spectra 6: an example of freshly annealed zeolite after exposure to  $\text{NO}_2$  vapor ( $4 \times 10^8$  L) at 300 K.



2 Torr for 180 s at 300 K. This data is shown in the inset labeled spectra 6 and indicates very efficient nitration relative to the surface containing adsorbed acetaldehyde molecules. These results do not rule out the importance of temperature, but clearly show that the accessibility of the surface sites is absolutely necessary.

At 375 K, most of the acetaldehyde desorbs from the zeolite (spectrum 3) and after the  $\text{NO}_2$  dosing at 2 Torr for 180 s, the characteristic spectrum of  $\text{NO}_2^-$  anions is observed (spectra 4 and 5). In order to prevent or at least minimize possible desorption and loss of volatile reaction products due to evacuation, spectrum 4 was obtained before pumping-out the system, i.e. some nitrogen dioxide was still present in the gas phase. It should be mentioned that the amount of nitrate compared to nitrite formed under these conditions is considerably lower than in the case of  $\text{NO}_2$  dosing on the clean zeolite surface. Some weak additional features at 590, 1560 and  $1610\text{ cm}^{-1}$  are observed after dosing  $\text{NO}_2$  on the surface that was heated to 375 K. These bands indicate the possible formation of  $\text{R-NO}_2$  (organic nitro),  $\text{R-ONO}$  (organic nitrite) and  $\text{R-NO}_3$  (organic nitrate) or  $\text{R-ONO}_2$  type species and are also consistent with the presence of adsorbed  $\text{NO}_2$ .

The interaction of  $\text{NO}_2$  with adsorbed acetaldehyde on partially covered zeolite surface was studied at 350 K and the results are presented in Fig. 6A. The sample was exposed to acetaldehyde vapor at 0.2 Torr for 180 s and then evacuated for 30 min at 0.005 Torr until the amount of adsorbed acetaldehyde remained constant in time (spectrum

1). Only the most intense bands corresponding to the aldehyde group ( $1720\text{ cm}^{-1}$ ) and  $\text{CH}_3$ -group bending vibrations ( $1350\text{ cm}^{-1}$ ) are observed.  $\text{NO}_2$  was then dosed into the system at 0.2 Torr for 180 s (spectrum 2) and the system was pumped back to 0.005 Torr. Spectra 3 and 4 correspond to 120 and 300 s of evacuation at 350 K. Exposure to  $\text{NO}_2$  triggers two main events with very different reaction rates. The first is the fast formation of surface  $\text{NO}_3^-$  groups with absorption bands at  $1350\text{--}1400\text{ cm}^{-1}$  and some nitro-compounds, probably embedded into the zeolite structure, with an absorption band at  $1150\text{--}1200\text{ cm}^{-1}$ . Note these processes are similar to those observed on “clean” zeolite surfaces. The second group of reactions is relatively slow and involves the transformation of the initially formed nitrate anions into nitrite ions. This is indicated by the decrease of the  $1350\text{--}1400\text{ cm}^{-1}$  band and the growth of the  $\text{NO}_2^-$  feature at  $1260\text{ cm}^{-1}$ . At the same time, there is a significant increase of  $1640$ ,  $1560$ ,  $1160$  and  $590\text{ cm}^{-1}$  bands.

#### 3.4.2. The role of organic nitro and organic nitrates

In order to understand the nature of the slow transformation and the production of features at  $1640$ ,  $1560$ ,  $1160$  and  $590\text{ cm}^{-1}$ , we have also examined the interaction of nitromethane ( $\text{CH}_3\text{NO}_2$ ) and isopropyl nitrate ( $\text{C}_3\text{H}_7\text{NO}_3$ ) with Na-Y zeolite at 300 K. The production of these molecules is expected in low-temperature plasmas and they have been implicated as potential reaction intermediates. These data are shown as transmission (absorption) spectra in Fig. 6B. In addition, the pure nitromethane absorption spectrum in the liquid state is shown in Fig. 6B for the sake of comparison. There is a remarkable correspondence of the spectra of adsorbed nitromethane and isopropyl nitrate with the features that emerge when dosing Na-Y containing some adsorbed acetaldehyde with  $\text{NO}_2$  at 350 K. Specifically, there is strong doublet observed around  $1600\text{ cm}^{-1}$ , a weak feature around  $1160\text{ cm}^{-1}$  and another moderately strong feature near  $590\text{ cm}^{-1}$ . The strong feature at  $1640\text{--}1660\text{ cm}^{-1}$  is typical of the C-ONO feature of an organonitrite ( $\text{R-ONO}$ ) compound. The weak feature near  $1160\text{ cm}^{-1}$  can be assigned to the mono-dentate nitrito species ( $\text{M-O-N-O}^-$ ), whereas the low frequency vibration near  $600\text{ cm}^{-1}$  may be associated with a phonon or bending feature of the  $[\text{-Al-O-Si-O-Al-}]^{2-}$  structure within the zeolite lattice. Though metal-oxygen stretching vibrations are typically in the  $700\text{--}300\text{ cm}^{-1}$  range, this could also be assigned as a bending feature of adsorbed  $\text{R-NO}_2$  or  $\text{R-ONO}$ . We note that this feature is not apparent for nitromethane ( $\text{CH}_3\text{NO}_2$ ) and isopropyl nitrate ( $\text{C}_3\text{H}_7\text{NO}_3$ ) adsorbed on silica (not shown) and is not present in the neat form of either nitromethane or isopropyl nitrate. Though this low frequency region is rarely studied, the  $600\text{--}590\text{ cm}^{-1}$  feature seems to indicate that the Al and the acid sites associated with it may be very important to the formation and/or reaction of organic nitro or organic nitrate type species on the surface. Indeed, plasma-activated treatment or reduction of  $\text{NO}_x$  in the presence of aldehy-

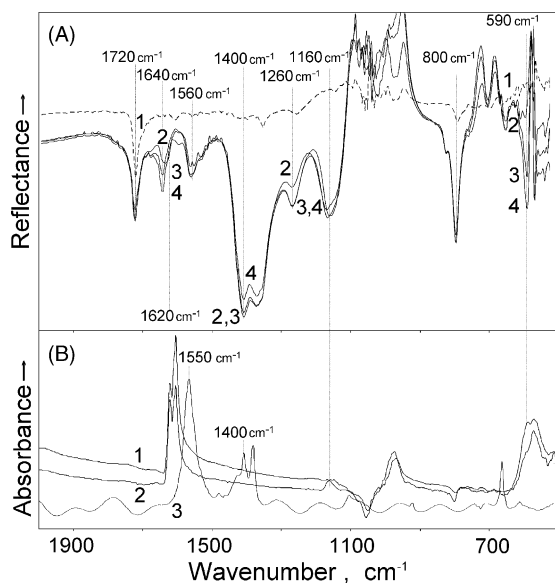


Fig. 6. A: Nitrogen dioxide reaction with the acetaldehyde pre-covered Na-Y zeolite at 350 K: Spectra 1 – initial sample with adsorbed acetaldehyde (dose  $4 \times 10^7$  L). Spectra 2 – the sample after stage(1) was exposed to  $4 \times 10^7$  L of nitrogen dioxide. Spectra (3) and (4) – the sample after 180 s and 300 s of evacuation Figure 6B: Transmission spectra of nitromethane (1), isopropyl nitrate (2) adsorbed on Na-Y zeolite at 300 K. Spectrum 3 shows the neat spectrum of liquid nitromethane.

des has been demonstrated on  $\gamma$ -alumina albeit at a much higher temperature than what we have examined [10,11].

It is also important to note that the strong feature between 1300 and 1500  $\text{cm}^{-1}$  for neat isopropyl nitrate and nitromethane is completely absent for the adsorbed species. The hydrocarbons bands at 1300–1500  $\text{cm}^{-1}$  are usually associated with C–H stretching vibrations of  $-\text{CH}_3$  and  $-\text{CH}$  groups. Their loss in the spectra of the molecules in the adsorbed state implies efficient oxidation or dehydrogenation of these groups at the surface. This also can imply loss of integrity of the hydrocarbon backbone. Thus, the important adsorbate is likely to be a nitrogen, carbon and oxygen containing molecule but this is not necessarily the parent molecule. We see no discernible features in the 2000–3000  $\text{cm}^{-1}$  region, thus, we do not support nor refute the suggestion that the species such as CNO ( $-\text{NCO}$ ) or HCN are important intermediates [19]. The interesting feature at 1560  $\text{cm}^{-1}$  observed in Fig. 6A is also absent in the spectra of adsorbed nitromethane and isopropyl nitrate. This frequency is often associated with an adsorbed C– $\text{NO}_2$  or C–N– $\text{NO}_2$  species and it has been observed in previous studies of the reaction of ozone treated *n*-hexane soot particles with  $\text{NO}_2$  [20].

The results clearly show that the reaction of  $\text{NO}_2$  with adsorbed organics leads to the formation of species that resemble those produced by directly dosing the zeolite surface with nitromethane and/or isopropyl nitrate. Thus, the results support the general conjecture that organic nitro/nitroso or organic nitrate compounds are indeed involved in the catalytic reduction of  $\text{NO}_x$ . It has been suggested that nitroso compounds can undergo spontaneous isomerization to oximes. In the cases studied here, such an isomerization could form an acetone oxime that could react further with  $\text{NO}_2$  to form  $\text{N}_2$ ,  $\text{N}_2\text{O}$ ,  $\text{CO}$ ,  $\text{CO}_2$  and  $\text{H}_2\text{O}$  [21]. Details of the complete reaction sequence leading to the formation of  $\text{N}_2$  are still unclear. Our results indicate that  $\text{NO}_2$  reacts with a surface adsorbed species and produces a deposit ostensibly the same as that produced by direct dosing of organic nitrites and nitrates. Perhaps the simplest reaction of  $\text{NO}_2$  with a hydrocarbon is the formation of HONO. This product can lead to the formation of diazonium and diazo compounds that thermally decompose to form  $\text{N}_2$ .

#### 4. Conclusions

We have examined the interaction of  $\text{NO}_2$  and  $\text{CH}_3\text{CHO}$  with Na-Y zeolite under conditions relevant to low-temperature plasma-activated reduction of  $\text{NO}_x$ . Acetaldehyde interacts weakly with the surface primarily via electrostatic and ion–dipole interactions and is not present at appreciable levels in the molecular adsorbed state at temperatures exceeding 350 K. The interaction of  $\text{NO}_2$  with Na-Y zeolite produces various forms of adsorbed nitrogen oxide species that are primarily present in the form of nitrites and nitrates. The nitrites can be present in the nitrito ( $-\text{O}-\text{N}-\text{O}^-$ ) and nitro ( $-\text{NO}_2^-$ ) configurations and nitrates in the ( $-\text{NO}_3^-$ )

and nitrate ( $-\text{O}-\text{NO}_2^-$ ) configurations. Reactions of  $\text{NO}_2$  with a Na-Y zeolite surface containing pre-adsorbed acetaldehyde at room temperature are primarily limited to oxidation of the organic fragments and reduction of the surface nitrates to surface nitrites. Reactions of  $\text{NO}_2$  on Na-Y zeolite surfaces containing a low coverage of acetaldehyde at temperatures  $>350$  K produces a dehydrogenated surface adsorbed species that likely contains C, N and O. This deposit strongly resembles what is produced when the surface is directly dosed with nitromethane and isopropyl nitrate. The surface reactions seem to involve the Al and associated acid sites. The chemical and structural identity of this deposit remains unknown. Our results neither support nor refute the concept that it is an isocyanate ( $-\text{NCO}-$ ) type intermediate.

#### Acknowledgements

This work was financially supported by Ford Motor Company. The authors thank Mark Saxon for his assistance with several of the experiments. Thom Orlando and John Hoard also wish to re-iterate their sentiments concerning Dr. Bernie Penetrante's very influential role in the development and understanding of plasma-activated catalysis. He will be greatly missed by all members of this community.

#### References

- [1] B.M. Penetrante, S.E. Schultheis (Eds.), *Nonthermal Plasma Techniques for Pollution Control*, Parts A and B, NATO ASI Series G: Ecological Sciences, Springer-Verlag, New York, 1993. ISBN 3-540-57174-4.
- [2] B.M. Penetrante, M.C. Hsiao, B.T. Merritt, G.E. Vogtlin, P.H. Wallman, M. Neiger, O. Wolf, T. Hammer, S. Broer, *Appl. Phys. Lett.* 68 (1996) 3719.
- [3] R.G. Tonkyn, S.E. Barlow, T.M. Orlando, *J. Appl. Phys.* 80 (1996) 9.
- [4] B.M. Penetrante, M.C. Hsiao, B.T. Merritt, *Trans. Plasma Sci.* 23 (1995) 679.
- [5] M.C. Hsiao, B.T. Merritt, B.M. Penetrante, R.G. Tonkyn, T.M. Orlando, *J. Oxid. Technol.* 1 (1996) 79.
- [6] R.G. Tonkyn, S.E. Barlow, M.L. Balmer, T.M. Orlando, J. Hoard, D. Goulette, *Society of Automotive Engineers Paper No.* 971716, 1997.
- [7] M.L. Balmer, R. Tonkyn, A. Kim, S. Yoon, D. Jimenez, T. Orlando, S.E. Barlow, J. Hoard, *Society of Automotive Engineers Paper No.* 982511, 1998.
- [8] M.L. Balmer, R. Tonkyn, A. Kim, S. Yoon, A. Kolwaite, S.E. Barlow, G. Maupin, T.M. Orlando, J. Hoard, *Society of Automotive Engineers Paper No.* 1999-01-3640, 1999.
- [9] H. Miessner, K.-P. Francke, R. Rudolph, Th. Hammer, *Catal. Today* 75 (2002) 325.
- [10] S. Yoon, A.G. Panov, R.G. Tonkyn, A.C. Ebeling, S.E. Barlow, M.L. Balmer, *Catal. Today* 72 (2002) 243.
- [11] S. Yoon, A.G. Panov, R.G. Tonkyn, A.C. Ebeling, S.E. Barlow, M.L. Balmer, *Catal. Today* 72 (2002) 251.
- [12] K. Shimizu, T. Oda, *IEEE Trans. Ind. Appl.* 35 (1999) 1311.
- [13] H.H. Kim, K. Takashima, S. Katsura, A. Mizuno, *J. Phys. D* 34 (2001) 604.
- [14] S.J. Schmieg, B.K. Cho, S.H. Oh, *Society of Automotive Engineers Paper No.* 2001-01-3565, 2001.

- [15] A.G. Panov, R.G. Tonkyn, M.L. Balmer, C.H.F. Peden, A. Malkin, J.W. Hoad, Society of Automotive Engineers Paper No. 2001-01-3513, 2001.
- [16] B.M. Penetrante, M.C. Hsiao, B.T. Merritt, G.E. Vogtlin, P.H. Wallman, A. Kuthi, C.P. Burkhart, J.R. Bayless, *Appl. Phys. Lett.* 67 (1995) 3096.
- [17] R. Dorai, K. Hassouni, M. Kushner, *J. Appl. Phys.* 88 (2000) 6060.
- [18] K. Hadjiivanov, *Catal. Rev.* 42 (2000) 77.
- [19] M. Haneda, Y. Kintaichi, M. Inaba, H. Hamada, *Catal. Today* 42 (1998) 127.
- [20] M.S. Akhter, A.R. Chughtai, D.M. Smith, *Appl. Spectrosc.* 45 (1991) 653.
- [21] H.-Y. Chen, T. Voskoboinikov, W.M.H. Sachtler, *J. Catal.* 180 (1998) 171.